Real-space multiple-scattering analysis of X-ray absorption near-edge K spectra of Cu_2O and CuO

1992 J. Phys.: Condens. Matter 4 9389

(http://iopscience.iop.org/0953-8984/4/47/019)

J. Phys.: Condens. Matter 4 (1992) 9389–9400. Printed in the UK

Real-space multiple-scattering analysis of x-ray absorption near-edge K spectra of Cu_2O and CuO

Ondřej Šipr

Institute of Physics, Czechoslovak Academy of Science, Cukrovarnická 10, 162 53 Praha 6, Czechoslovakia

Received 22 June 1992, in final form 10 September 1992

Abstract. X-ray absorption near-edge structure of Cu K spectra of Cu_2O and CuO are analysed within the real-space multiple-scattering formalism. The crudest approximation (both in the cluster size and in the order of scattering) which can be made so that a particular spectral feature is still satisfactorily reproduced is found for each of the peaks. It was demonstrated that the peaks which correspond to one another both in the energy position and in the magnitude need not arise through the same scattering mechanism. Hence, caution must be exercised when the spectra of different compounds are compared. Multiple scattering involving non-collinear atoms can be important even in materials with inversion symmetry at ~20 eV above the edge.

1. Introduction

X-ray absorption near edge structure (XANES) of Cu K spectra of Cu_2O and CuO often serve as a reference standard for the analysis of x-ray absorption spectra of high-T_c superconductors. Attempts were made to investigate the electron structure by comparing positions and intensities of corresponding peaks in spectra of different compounds (Alp *et al* 1987, Lyttle *et al* 1988, Tranquada *et al* 1988, Rao and Garg 1991). This progress stimulates the effort not only to calculate the spectra but also to understand the physical origin of their particular features.

Considerable effort has been devoted to the interpretation of Cu K spectra in copper compounds within the molecular orbital (MO) formalism in the past years (Bair and Goddard 1980, Kosugi *et al* 1984, Smith *et al* 1985, Yokoyama *et al* 1986). The basic idea underlying this approach is that a correspondence between the atomic and the crystal energy levels can be established. The spectral features are interpreted in terms of transitions of the core electron to unoccupied states. The great advantage of this approach is that it associates particular peaks of the spectrum with well defined and well understood quantities (such as atomic energy levels). Its disadvantage is that it relies on calculations performed for a small molecular cluster—it is not clear, whether such results can be transferred to solids without substantial corrections.

The real-space multiple-scattering (RS-MS) formalism is another technique which proved to be an efficient tool for XANES calculation in the past decade. Within this approach, the absorption cross-section is calculated as a (formally infinite) sum of terms, each of them representing a particular 'scattering path' of the excited photoelectron between individual atoms (see e.g. Durham 1988). All unoccupied states are treated as

0953-8984/92/479389+12$07.50

belonging to the continuum. Although only a finite number of atoms can be involved (similarly to the MO approach), existing programs are able to consider as many as ~100 atoms so that full convergence can be achieved. The RS–MS formalism is well suited to introducing various approximations both in the cluster size and in the order of scattering involved.

The investigation of the effect of the cluster size on the shape of the spectrum constitutes now an almost standard part of a RS–MS formalism-based study of XANES (cf Garg *et al* 1988, Li *et al* 1991, Bianconi *et al* 1991). On the contrary, evaluation of the importance of various types of multiple scattering (MS) proved to be a difficult task in the past and it has become a subject of a vivid discussion (Bunker and Stern 1984, Vvedensky and Pendry 1985, Benfatto *et al* 1986, Bouldin *et al* 1988). To the author's knowledge, there has not been published any study quantifying the role of individual scattering paths in the XANES cross-section so far. In fact, doubts can be raised about the wisdom of such an analysis as there are some hints that even relatively significant scattering paths (according to their individual transition amplitude) may not contribute to the total cross-section because of their mutual cancellation (Benfatto *et al* 1988, Šipr 1990). It seems plausible to deal rather with whole sets of scattering paths than to treat them individually. One can try to find out which approximations can be made so that the original spectrum is still reproduced. Looking for a physical interpretation of a particular spectral feature means in this context to find the 'crudest acceptable approximation' (CAA), i.e. the crudest approximation (both in the cluster size and in the order of scattering) which can be made, so that the relevant feature would still not disappear. This information should serve as a clue to understanding the role of individual atoms in the formation of XANES.

Recently, the concept of the 'trapping time' was introduced by Guo *et al* (1989) to quantify the time the photoelectron spends in the vicinity of a particular atom. This approach was applied to Cu_2O and CuO by Guo *et al* (1990). Hence, it would be useful to compare their results with the findings of the CAA analysis.

The aim of this paper is to calculate the XANES spectra of Cu_2O and CuO within the RS–MS formalism and to look for the CAA for each spectral peak. Such an assignment should serve as a guide for finding the physical interpretation of the spectra and at the same time as a test as to whether the concept of CAA can be useful in XANES analysis. A comparison with the trapping time analysis of Guo *et al* (1990) will be made.

2. Method of calculation

2.1. Approximations to multiple scattering

The polarization-averaged XANES spectra were calculated by a modification of the ICXANES computer code of Vvedensky *et al* (1986). The whole cluster of atoms is divided into the central atom (i.e. the atom from which the photoelectron was emitted) and the outer cluster, which is further decomposed into several concentric shells. The intrashell (between atoms belonging to the same shell) as well as the intershell (between atoms belonging to different shells) scattering are calculated separately. Hence, different approximations to different types of scattering can be introduced.

The calculation of XANES proceeds in three steps. First, the intrashell part of the calculation is performed and the shell scattering matrices characterizing the reflection and the transmition properties of a particular shell are found. For the purpose of finding the CAA, three orders of approximation are distinguished in this step : (i) full

intrashell MS (denoted as f in the following), (ii) double intrashell scattering (d) and finally (iii) single intrashell scattering (s). The second (intershell) step consists in calculating the total reflection matrix of the outer cluster. This is accomplished by a recursive calculation of the joint reflection matrix of the outermost pair of the shells, thus effectively reducing their number by one until the innermost one is included. Again, three orders of approximation are introduced: (i) full intershell MS (denoted as F), (ii) the lowest-order renormalized forward scattering (R) and (iii) single intershell scattering (S). The definition of renormalized forward scattering (RFS) together with relevant equations can be found in Vvedensky *et al* (1986). Note that the lowest-order RFS accounts e.g. for the 'shadowing effect' (Lee and Pendry 1975). Finally, after the total reflection matrix is formed, the scattering of the electron between the central atom and the outer cluster is considered either within the single scattering approximation (S) (only scattering paths which do not pass more than once through the central atom are included) or within the full MS mode (F).

In contrast to the original ICXANES program, the modified code enables one to choose different orders of approximation to the intershell scattering for different neighbouring pairs of shells. Each particular calculation is denoted by a sequence of letters indicating the approximations involved in it (the order of the letters corresponds to progress from the central atom outwards). Hence, e.g. the symbol [S f F d R s] means that the following scattering terms were included: single scattering between the central atom and the outer cluster (S), full intrashell MS within the first shell (f), full intershell MS between the first shell and the outer shells (F), double intrashell scattering within the second shell (d), the lowest-order intershell RFS between the second shell and the outer shell (R) and single intrashell scattering within the third shell (s).

2.2. *Construction of scattering potential*

A non-self-consistent muffin-tin potential was constructed by superposing atomic charge densities (Mattheiss 1964). The atomic charge densities were calculated within the local density approximation by a program of Vackář (1988), the Kohn-Sham exchange parameter $\alpha = 2/3$ was used. The core-hole was taken into account by removing one 1s electron from the central Cu atom and putting it into its lowest unoccupied level ('relaxed and screened model'). The muffin-tin radii were chosen so that there would be no potential discontinuities at the touching points. The muffin-tin zero (MTZ) was found by averaging the potential in the interstitial region.

Such a construction of MTZ produces a jump in the potential at the boundaries of muffin-tin spheres (up to 0.33 H for Cu_2O and up to 0.18 H for CuO, respectively). Unlike some other authors (Garg *et al* 1988), the present author did not follow the proposition of Holland *et al* (1978) to subtract a constant from MTZ to remove this discontinuity since no physical interpretation of such a procedure has been given so far. The fact that the resulting spectra (see section 3) are in a good agreement with both experiment and previous calculations (Norman *et al* 1985) indicates that the potential was accurate enough and that no 'false oscillations' (Holland *et al* 1978) occurred.

The maximum angular momentum quantum number used in the atomic scattering calculation was $\ell_{max} = 3$. Such a restriction could influence the positions of high-energy peaks. In order to test this, XANES spectra of Cu_2O for a 21-atom cluster and of CuO for a 11-atom cluster were calculated for both $\ell_{max} = 3$ and $\ell_{max} = 4$. The corresponding curves were found to be identical within the thickness of the line for energies up to 40 eV above the edge.

3. Results

3.1. Cu_2O

The structure of Cu_2O was taken from Wycoff (1963). The nearest neighbourhood of Cu consists of two axial O atoms at the distance of 3.49 au, then comes a shell of twelve Cu atoms at 5.71 au followed by six O atoms at of 6.69 au The crystal has an inversion symmetry with respect to the central Cu atom. The perspective diagram of the nearest neighbourhood of Cu in Cu_2O is shown in figure 1.

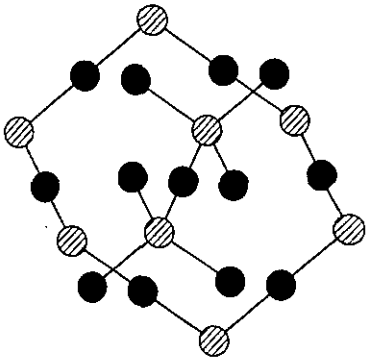

Figure 1. Perspective diagram of the nearest neighbourhood of Cu atom in Cu_2O (the $Cu_1(O_2)(Cu_{12})(O_6)$ cluster shown). The Cu atoms are represented by full circles, the O atoms by hatched circles. The rods connect atoms of mutual distance of 3.49 au

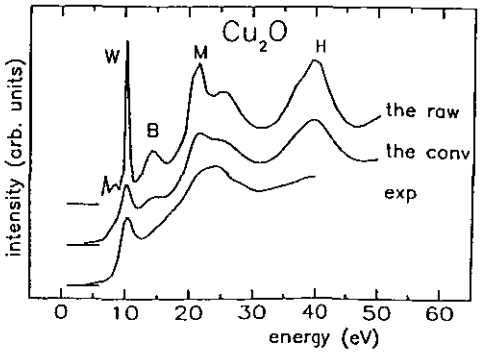

Figure 2. Comparison of experimental and theoretical spectra of Cu_2O. The experimental curve is from Lyttle *et al* (1988). See text for details.

A comparison of the theory with the experiment is presented in figure 2. The zero of the energy scale is at MTZ, the experimental spectrum of Lyttle *et al* (1988) was aligned so that the positions of the peak W ('white line') would coincide. The theoretical curve was obtained for a cluster of 77 atoms divided into four shells, $Cu(Cu_{12}O_2)(Cu_6O_{12})(Cu_{24})(Cu_{12}O_8)$. Full MS is considered for $E \leqslant 19$ eV, the [F f F f F f R d] mode (i.e. full MS except for the lowest-order RFS between the third and the fourth shell and for the double intrashell scattering within the fourth shell) is applied for higher energies. The maximum angular momentum number employed in the decomposition of the scattering into its intra- and intershell parts (Durham *et al* 1982, Durham 1988) was $\ell_{out} = 22$ for $E \leqslant 19$ eV and $\ell_{out} = 20$ for $E > 19$ eV. The results were tested for convergence both in the cluster size and in ℓ_{out}.

In order to suppress the redundant structure in the spectra, the theoretical data were convoluted by a lorentzian curve of the energy-dependent full width at half maximum (FWHM) $w = 1.5 + 0.04(E - 8.5)$ [eV]. The energy-independent part of w corresponds to the finite life time of the 1s Cu core hole, the energy-dependent part accounts for the finite lifetime of the excited photoelectron due to its inelastic scattering (note that 8.5 eV is the approximate position of the absorption edge relative to MTZ). Such a choice is analogous e.g. to the procedures applied by Bianconi *et al* (1991), Li *et al* (1991) or Speier *et al* (1985). As it was not the goal of this paper to achieve the best visual

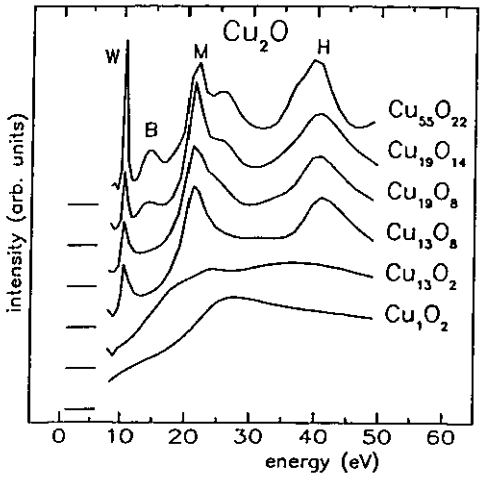

Figure 3. Effect of the size of the cluster on XANES spectrum of Cu_2O. The sizes of the clusters involved are (from top to bottom): $Cu_{55}O_{22}$, $Cu_{19}O_{14}$, $Cu_{19}O_8$, $Cu_{13}O_8$, $Cu_{13}O_2$ and CuO_2.

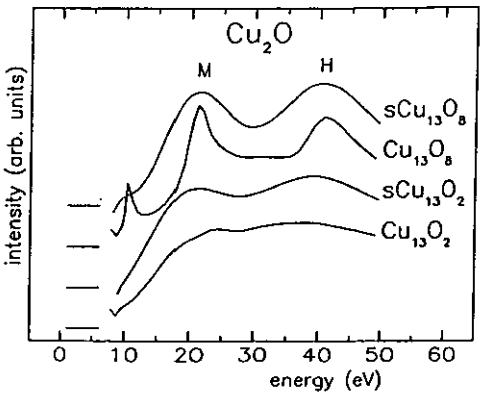

Figure 4. Investigation of the origin of the peaks M, H in XANES of Cu_2O. The curves correspond to (from top to bottom): SS calculation for a $Cu_{19}O_8$ cluster, full MS calculation for a $Cu_{19}O_8$ cluster, SS calculation for a $Cu_{13}O_8$ cluster and full MS calculation for a $Cu_{13}O_8$ cluster.

agreement between the theory and the experiment, no attempts to find a more suitable FWHM were made.

The effect of the cluster size is shown in figure 3. All the curves but the uppermost one were calculated employing full MS, the uppermost curve (denoted $Cu_{55}O_{22}$) is identical with the raw theoretical curve of figure 2. It is evident that the nearest neighbourhood alone (two O atoms) cannot give rise to the observed structure. The peaks M ('main') and H ('high-energy') are slightly indicated for the $Cu_{13}O_2$ cluster and fully developed for the $Cu_{13}O_8$ cluster. At this size of the cluster also the W peak appears. A cluster as large as $Cu_{19}O_{14}$ is required for the reproduction of the peak B ('bump').

Next comes the investigation of the origin of individual peaks. The peaks M and H are predominantly of a single-scattering (SS) nature. This is demonstrated in figure 4 where both full MS and SS results are displayed for the $Cu_{13}O_2$ and $Cu_{13}O_8$ clusters. Inclusion of MS does not alter the SS curves near the peaks M and H significantly.

The peak W is reproduced for a $Cu_{13}O_8$ cluster (figure 3). At first, this cluster was divided into the central atom plus two shells—$Cu(O_2)(Cu_{12}O_6)$. The peak W is reproduced when the [S s F d] approximation is applied (figure 5). This approximation is also the crudest acceptable one: the double scattering within the second shell is essential (the position of W is incorrect when only SS is included—cf the [F f F s] curve), the full intershell MS between the first and the second shell is essential too, (the low-energy side of W falls below zero when only lowest-order RFS is included — cf the [F f R d] curve).

In order to learn more about the nature of W, it is necessary to divide further the second shell ($Cu_{12}O_6$). The analysis of XANES for the $Cu_{13}O_8$ cluster divided into three shells $Cu(O_2)(Cu_{12})(O_6)$ is shown in figure 6. As the CAAS concerning the first three 'letters' (scattering between the central atom and the outer cluster, intrashell scattering within the first shell, and intershell scattering between the first shell and the outer shells) are known from figure 5 (they are [S s F]), only the approximations occurring in the

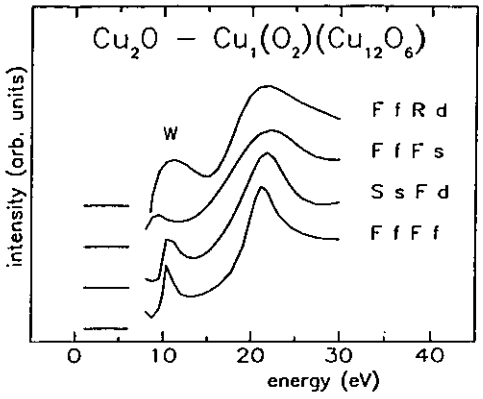

Figure 5. Search for the CAA for the peak W in Cu_2O spectrum. The curves correspond to calculations for a $Cu_{13}O_8$ cluster divided into two shells.

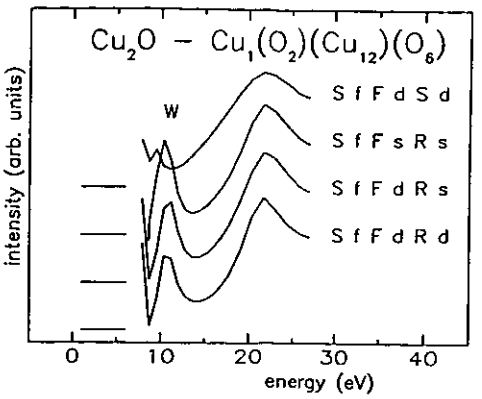

Figure 6. Search for the CAA for the peak W in Cu_2O spectrum. The curves correspond to calculations for a $Cu_{13}O_8$ cluster divided into three shells.

remaining steps (represented by the last three letters of the symbols labelling the curves in figure 6) are significant now. The [S f F d R s] curve reproduces W satisfactorily. Replacement of the double scattering within the (now) second shell by SS pushes the low-energy side of W below zero (the [S f F s R s] curve), replacement of the RFS between the second shell and the third one by SS causes even W to disappear. Hence, combining the results of figure 5 and figure 6, one can conclude that the CAA for the W peak is [S s F d R s] for the $Cu(O_2)(Cu_{12})(O_6)$ division of the $Cu_{13}O_8$ cluster.

3.2. CuO

The structure of CuO was taken from Åsbrink and Norrby (1970). The nearest neighbourhood of a Cu atom consists of four nearly planar O atoms (at a distance of 3.69 au or 3.71 au, respectively), which form a distorted pyramid with two apical O atoms at 5.26 au The four nearest Cu atoms at 5.48 au form a plane. The crystal has an inversion symmetry with respect to central Cu. The perspective diagram of the nearest neighbourhood of Cu in CuO is shown in figure 7.

A comparison of the theory with the experiment of Drahokoupil *et al* (1990) is presented in figure 8. The experimental spectrum was aligned so that the peaks M would coincide. The theoretical curve was obtained for a cluster of 77 atoms divided into six shells, $Cu(O_4)(Cu_{12}O_4)(Cu_2O_{14})(Cu_6O_8)(Cu_{10}O_4)(Cu_8O_4)$. Full MS is taken into account for $E \leqslant 22$ eV, while the [F f F f F f F f R d R d] approximation was used at higher energies. The maximal ℓ_{out} was 18. Checks for the convergence both in the cluster size and in ℓ_{out} were made. Again, the theoretical spectrum convoluted with a Lorentzian curve of the same FWHM as in figure 2 is displayed.

The cluster-size effect is studied in figure 9. All the curves but the uppermost one were calculated within the full MS mode, the uppermost one ($Cu_{39}O_{38}$) is identical with the uppermost curve of figure 8. The peak M can be reproduced if the nearest four neighbours are taken into account, the reproduction of the peak S ('shoulder') requires six nearest neighbours (CuO_6) to be included, the peak P ('pre-peak') appears in the Cu_5O_6 cluster spectrum for the first time. The peak H cannot be reproduced satisfactorily even by a cluster as large as $Cu_{13}O_8$.

The origin of the peak M is analysed in figure 10. The choice [S f] results in a

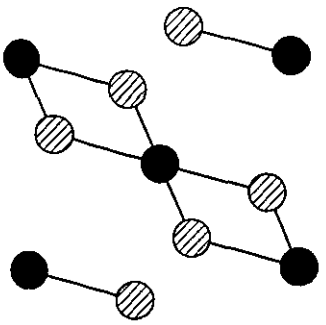

Figure 7. Perspective diagram of the nearest neighbourhood of Cu atom in CuO (the $Cu_1(O_4)(O_2)(Cu_4)$ cluster shown). The Cu atoms are represented by full circles, the O atoms by hatched circles. The rods connect atoms of mutual distance of 3.69 au or 3.71 au, respectively.

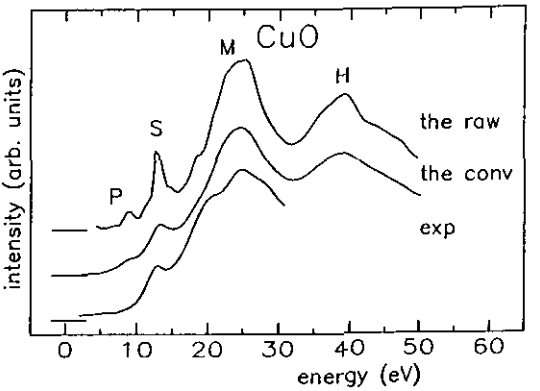

Figure 8. Comparison of experimental and theoretical spectra of CuO. The experimental curve is from Drahokoupil *et al* (1990).

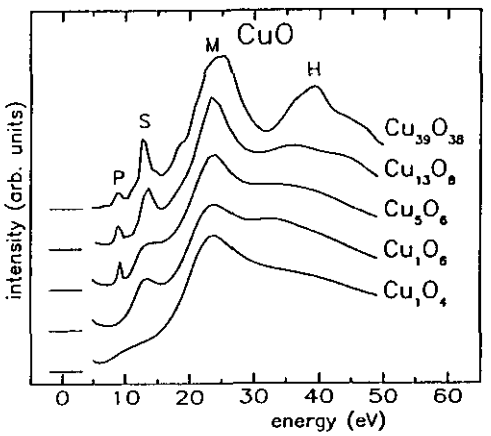

Figure 9. Effect of the size of the cluster on the XANES spectrum of CuO. The sizes of the clusters involved are (from top to bottom): $Cu_{39}O_{38}$, $Cu_{13}O_8$, Cu_5O_6, CuO_6 and CuO_4.

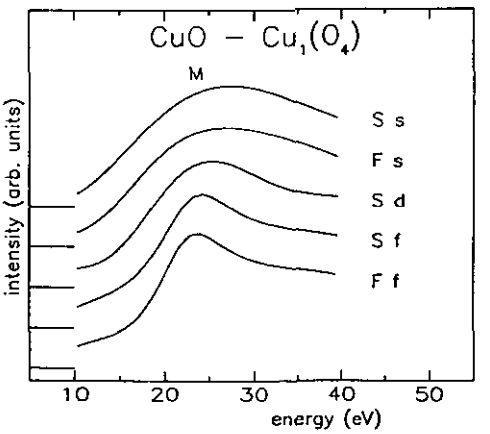

Figure 10. Investigation of the origin of the peak M in CuO. The curves correspond to calculations for a CuO_4 cluster.

spectrum nearly identical with the full MS curve, the choice [S d] leads to a 1.7 eV discrepancy in the position, the SS choice [S s] leads to a 3.5 eV disagreement. The [F s] curve hardly differs from the SS result. All this implies that the CAA for the peak M is [S f].

Figure 11 is devoted to the S peak. The CuO_6 cluster was divided into the central atom plus two shells, $Cu(O_4)(O_2)$. The CAA for the peak S is [S f R s]. Its acceptability follows from the second-lowermost curve; the two uppermost curves demonstrate that it is really the crudest of all the acceptable approximations. Replacement of the full MS within the first shell by double scattering results in disappearance of S, replacement of the RFS between the first shell and the second one by SS put S into an incorrect position (its low-energy tail reaches the region where the peak P is to appear).

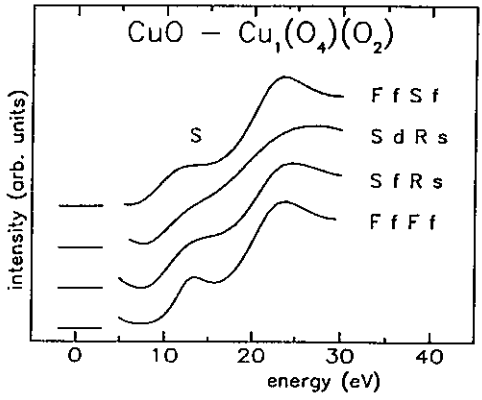

Figure 11. Investigation of the origin of the peak S in CuO. The curves correspond to calcualtions for a CuO_6 cluster.

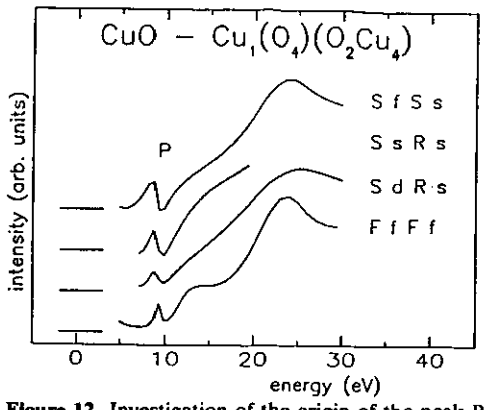

Figure 12. Investigation of the origin of the peak P in CuO. The curves correspond to calculations for a Cu_5O_6 cluster.

Figure 12 displays the spectra calculated for a Cu_5O_6 cluster. The outer cluster was divided into two shells, $Cu(O_4)(O_2Cu_4)$. The peak P is reproduced within the [S d R s] approximation. The replacement of the double scattering within the first shell by intrashell SS pushes the high-energy side of the peak P below zero (the curve [S s R s]), the same is true also for the replacement of the RFS between the first and the second shell by the intershell SS (the curve [S f S s]).

The curves displayed in figures 9–10 indicate that the peak M is formed by full intrashell scattering within the CuO_4 cluster. However, this conclusion could be questioned on the basis of figure 13, where the results of SS calculation for a sequence of clusters are shown. It is evident that the peaks M and H can be reproduced within the SS approximation provided that a sufficiently large cluster is taken into account. The question now arises of which mechanism of forming the M peak is dominant: MS within four nearest O atoms or SS from a large cluster of ~40 atoms.

The decision could come from consideration of the finite electron mean free path. One could guess that the curves in figures 9–10 overestimate MS by including implicitly very long scattering paths which would be damped in a real sample and that it is just this overestimation what causes the peak M to be reproduced within the CuO_4 cluster. In order to test this, model calculations for a Cu_5O_6 cluster were performed explicitly accounting for the finite mean free path. This was performed in a way common in EXAFS (extended x-ray absorption fine structure) calculations, namely by a multiplication of every propagator $g_{LL'}^{ij}$ (see Durham *et al* (1982) for the definitions) by an exponential damping factor $\exp[-R^{ij}/(2\lambda)]$, where R^{ij} is the distance between the scattering centres i, j and λ is the electron mean free path. Alternatively, the same effect could be achieved by introducing an imaginary part to the self-energy (Durham *et al* 1982). In order to suppress the redundant scattering paths as much as possible, λ was chosen so that it would correspond to a SS path from the central atom to the boundary of a five-atom CuO_4 cluster and back ($\lambda = 7.4$ au) and to a SS path to the boundary of an eleven-atom cluster and back ($\lambda = 11.0$ au). The results are displayed in figure 14. The peak M is well reproduced for both choices of λ, hence its reproducibility within the CuO_4 cluster cannot be a consequence of an overestimation of MS.

The question of which of the two mechanisms contributes to M more significantly can be partly resolved by comparing the heights of the M peak. In order to get the pure

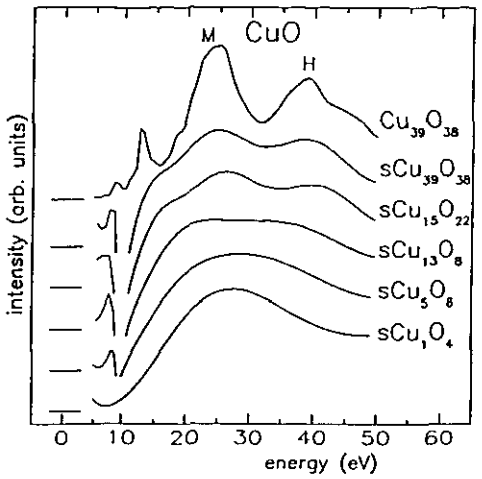

Figure 13. Cluster-size effect for a SS calculation of XANES of CuO. The uppermost curve corresponds to the full MS calculation for the $Cu_{39}O_{38}$ cluster, the other curves display SS results for the (from top to bottom) $Cu_{39}O_{38}$, $Cu_{15}O_{22}$, $Cu_{13}O_8$, Cu_5O_6 and CuO_4 clusters.

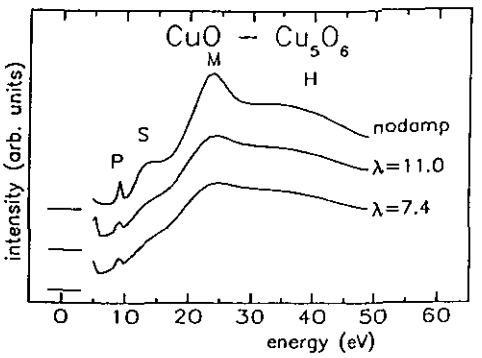

Figure 14. Effect of the finite electron mean free path λ on XANES spectrum of CuO. All curves display results for a Cu_5O_6 cluster. The uppermost curve corresponds to $\lambda = \infty$ (no damping included), the middle curve corresponds to $\lambda = 11.0$ au and the lowermost curve to $\lambda = 7.4$ au.

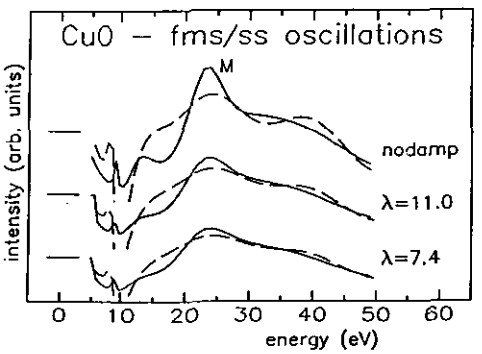

Figure 15. Comparison of spectral oscillations corresponding to a SS calculation for a $Cu_{39}O_{38}$ cluster (broken line) and to a MS calculation for a Cu_5O_6 cluster (full line). Again, the results for three choices of the electron mean free path are displayed ($\lambda = \infty$, $\lambda = 11.0$ au and $\lambda = 7.4$ au).

scattering contribution, an atomic-like XANES curve was subtracted from the Cu_5O_6-cluster full MS spectrum as well as from the $Cu_{39}O_{38}$-cluster SS spectrum. The results are displayed in figure 15. It is evident that near the peak M, MS within a small cluster (full line) is more important than SS within a large cluster (broken line), even though the significance of SS increases when the damping is included. Nevertheless, a more comprehensive analysis would be required to make this point more clear.

4. Discussion

It can be seen from figure 2 that the positions of the peaks W and M in the Cu_2O spectrum agree well with the experiment. The peak B can hardly be identified in the experimental curve of Lyttle et al (1988), though it is clearly visible in the Cu_2O experimental spectrum of Rao and Garg (1990). The position of the peak H in figure 2 is in a good agreement with the M–H distance of ~17 eV in the experimental spectrum

of Norman *et al* (1985). The theoretical curve of Norman *et al* (1985) looks different from the theoretical curve of figure 2 in the vicinity of the peaks W and B. As only a few details are available about the calculation of Norman *et al* (1985), no guess about the origin of this discrepancy can be made.

Predicted positions of the peaks S and M in the CuO spectrum (figure 8) agree well with the experiment of Drahokoupil *et al* (1990), the M–H distance agrees well with the experimental distance ~16 eV of Norman *et al* (1985). There is a relatively large discrepancy in the P–S distance (4 eV theory, 7 eV experiment). Two sources of this disagreement can be suggested: i) The present calculation relies solely on the dipole approximation while indications exist that the peak P corresponds to a quadrupole transition (Hahn *et al* 1982), and ii) band-structure results (Ching 1989) imply that the simple one-electron approach cannot describe the electron states close to the edge correctly in CuO. This suggests that the theoretical peak P may not correspond to the experimental peak P. Nevertheless, the peak P was also subdued to the CAA analysis because it could be interesting to learn more about the nature of MS in this region even if the relevant feature is overridden by some other effect.

Self-consistent MO calculations of Yokoyama *et al* (1986) and Kosugi *et al* (1984) demonstrate that the peak S corresponds to a multielectron shake-down process in a $CuCl_2{\cdot}2H_2O$ molecule or in a $CuCl_4^{2-}$ molecular complex. This indicates that such processes might be important in copper oxide crystals, too. One-electron RS–MS calculations (figure 8) show that many-electron processes are not necessary for the formation of S in CuO. However, they could be responsible for the fine structure of the M peak in CuO (see figure 8), although other causes (such as non-sphericity of the potential) cannot be excluded.

Table 1. Assignment of XANES features of Cu_2O compound spectrum resulting from the trapping time analysis based on a MO calculation for the $Cu_{13}O_8$ cluster. For more details, see table II of Guo *et al* (1990).

Feature	Interpretation
W	central Cu states perpendicular to the O–Cu–O axis
M	central Cu (dominant), axial O and 2nd shell O states
H	axial O and 2nd shell O states

Table 2. Assignment of XANES features of CuO compound spectrum resulting from the trapping time analysis based on a MO calculation for the Cu_5O_6 cluster. For more details, see table 3 of Guo *et al* (1990).

Feature	Interpretation
S	central Cu states oriented towards apical O atoms
M	central Cu (dominant) and planar O states
H	planar O and apical O states

The XANES interpretation based on the trapping time analysis of Guo *et al* (1990) is summarized in tables 1 and 2. There is a general agreement concerning the interpretation of the peaks M and H in Cu_2O (cf table 1 and figures 3 and 4) and of the peak M in CuO (table 2 and figures 9 and 10). The trapping time interpretation of

S in CuO as arising from the states oriented towards the apical O atoms is consistent with the appreciation of the role of these atoms in figures 9 and 11, too. A disagreement arises in case of the peaks W in Cu_2O and H in CuO: the reproduction of W within the RS–MS formalism demands that the scattering from the whole $Cu_{13}O_8$ cluster must be included (figures 3, 5 and 6), which is in contrast to the dominance of central Cu states resulting from the trapping time analysis (table 1). Similarly, the reproduction of the H peak in CuO requires that a much larger cluster than CuO_6 must be involved (cf figure 9 and table 2).

It is not clear whether this disagreement is of a physical origin or not. Namely, the sequences of spectral curves displayed in figures 3 and 9 inform only about the size of the minimum region which it is necessary to take into account so that a particular peak can be reproduced. The spatial probability distribution of the photoelectron is not known since wave functions were not calculated by the present author. In contrast, the analysis of Guo *et al* (1990) relies on wave functions and informs about the true probability distribution. Hence, a different interpretation in terms of the CAA and the trapping time analysis need not mean a real contradiction.

Sinha *et al* (1990) investigated the origin of the peak S employing the correlation between the energy separation E and interatomic distance R, $\sqrt{E}\,R$ = constant, proposed first by Natoli (1983). Their conclusion—that S arises due to MS within the nearest four oxygen atoms—is not quite incorrect but it is incomplete: figures 9 and 11 demonstrate that although the four planar O atoms play an important role, the two apical O atoms cannot be omitted.

The present paper questions the procedure Lyttle *et al* (1988) used for XANES analysis of Cu compounds. Their E versus R correlation curves are based on such an identification of peaks with particular lattice sites which is in sharp disagreement with the identification resulting from section 3. of this paper. For example they suppose that the M peak in CuO is created by two apical O atoms (contrary to four planar O atoms as suggested by figures 9–10) and that the peak and H arises from the nearest O planar atoms (contrary to figure 10 which suggests that at least ~20 atoms are necessary to reproduce it). Indeed, a close look at figures 4 and 9 of Lyttle *et al* (1988) reveals that the assumed correlation between atomic distances and peak positions is not very convincing.

The CAA for the peak M in CuO was found to be [S f] for the $Cu(O_4)$ cluster (figure 10). This means that MS paths among non-collinear atoms, i.e. of type two according to the terminology of Bunker and Stern (1984), must be included. This is surprising as it was a general belief that type two scattering would be negligible in materials with inversion symmetry due to mutual cancellations (Bunker and Stern 1984). The finding that type two MS must be included at ~20 eV above the edge in CuO does not contradict directly to conclusions estimating that the ratio of the MS amplitude to SS amplitude should be small. Rather, it points out that the numerical negligibility need not imply the 'observational' negligibility and that even a relatively small MS amplitude may produce a clearly distinguishable effect (cf figures 1 and 3 of Bouldin *et al* 1988).

5. Conclusion

The present paper demonstrates that particular peaks in XANES spectra need not have the same physical origin even though they correspond to each other in the energy scale (e.g. the main peak M is formed by the nearest neighbourhood in CuO but not in Cu_2O).

Hence, caution ought to be exercised whenever far-reaching conclusions are made from comparison of XANES spectra of different compounds. It is reasonable to look for the crudest acceptable approximation necessary for the reproduction of every individual peak. The idea of CAA seems to be consistent with the trapping time analysis of Guo *et al* (1990), nevertheless one should be aware of the fact that both approaches rely on different concepts. Type two multiple scattering can be important as far as ~20 eV above the edge even for environments with an inversion symmetry.

Acknowledgments

The author is grateful to the ASCOC Laboratory, Prague, where most of the calculations were performed.

References

Åsbrink S and Norrby L-J 1970 *Acta Crystallogr.* B **26** 8
Bair R A and Goddard III W A 1980 *Phys. Rev.* B **22** 2767
Benfatto M, Natoli C R, Bianconi A, Garcia J, Marcelli A, Fanfoni M and Davoli I 1986 *Phys. Rev.* B **34** 5774
Bianconi A, Li C, Campanella F, Della Longa S, Pettini I, Pompa M, Turtù S and Udron D 1991 *Phys. Rev.* B **44** 4560
Bouldin C E, Bunker G, McKeown D A, Forman R A and Ritter J J 1988 *Phys. Rev.* B **38** 10 816
Bunker G and Stern E A 1984 *Phys. Rev. Lett.* **52** 1990
Ching W, Xu Y N and Wang K W 1989 *Phys. Rev.* B **40** 7684
Drahokoupil J, Polčík M and Pollert E 1990 *Solid State Commun.* **74** 773
Durham P J 1988 *X-ray Absorption: Principles, Applications, Techniques of EXAFS, SEXAFS and XANES* ed D C Koningsberger and R Prins (New York: Wiley) p 53
Durham P J, Pendry J B and Hodges C H 1982 *Comput. Phys. Commun.* **25** 193
Garg K B, Bianconi A, Della Longa S, Clozza A and De Santis M 1988 *Phys. Rev.* B **38** 244
Guo J, Ellis D E, Alp E E, Soderholm L and Shenoy G K 1989 *Phys. Rev.* B **39** 6125
Guo J, Ellis D E, Goodman G L, Alp E E, Soderholm L and Shenoy G K 1990 *Phys. Rev.* B **41** 82
Hahn J E, Scott R A, Hodgson K O, Doniach S, Desjardins S R and Solomon E I 1982 *Chem. Phys. Lett.* **88** 595
Holland B W, Pendry J B, Pettifer R F and Bordas J 1978 *J. Phys. C: Solid State Phys.* **11** 633
Kosugi N, Yokoyama T, Asakura K and Kuroda H 1984 *Chem. Phys.* **91** 249
Lee P A and Pendry J B 1975 *Phys. Rev.* B **11** 2795
Li C, Pompa M, Congiu Castellano A, Della Longa S and Bianconi A 1991 *Physica* C **175** 369
Lyttle F W, Greegor R B and Panson A J 1988 *Phys. Rev.* B **37** 1550
Mattheiss L F 1964 *Phys. Rev.* **133** A1399
Natoli C R 1983 *EXAFS and Near Edge Structure* ed A Bianconi, L Incoccia and S Stipcich (Berlin: Springer) p 43
Norman D, Garg K B and Durham P J 1985 *Solid State Commun.* **56** 895
Rao K V R and Garg K B 1991 *Physica* C **178** 352
Sinha R N, Mahto P and Chetal A R 1990 *Z. Phys.* B **81** 229
Šipr O 1990 unpublished
Smith T A, Penner-Hahn J E, Berfing M A, Doniach S and Hodgson K O 1985 *J. Am. Chem. Soc.* **107** 5945
Speier W, Zeller R and Fuggle J 1985 *Phys. Rev.* B **32** 3597
Tranquada J M, Heald S M, Moodenbaugh A R and Xu Youwen 1988 *Phys. Rev.* B **38** 8893
Vackář J 1988 unpublished
Vvedensky D D, Saldin D K and Pendry J B 1986 *Comput. Phys. Commun.* **40** 421
Wycoff R W G 1963 *Crystal Structures* vol 1 (New York: Wiley)
Yokoyama T, Kosugi N and Kuroda H 1986 *Chem. Phys.* **103** 101